**PALEOBIOLOGY**
A PUBLICATION OF THE **Paleontological SOCIETY**

**CAMBRIDGE UNIVERSITY PRESS**

# Corallite sizes of reef corals: decoupling of evolutionary and ecological trends

Danijela Dimitrijević 🆔, Nussaïbah B. Raja 🆔 and Wolfgang Kiessling 🆔

GeoZentrum Nordbayern, Friedrich-Alexander-Universität Erlangen-Nürnberg, 91054 Erlangen, Germany;
Email: nussaibah.raja.schoob@fau.de; wolfgang.kiessling@fau.de

## Non-technical Summary

Reef-building corals live with algae in their tissues. They form a mutually beneficial relationship called photosymbiosis, wherein algae provide corals with nutrients, and in return, the coral provides the algae with protection. Even though corals obtain a majority of their nutrients through algae, they also catch and feed on prey such as plankton. Today we can observe a relationship between the size of the coral polyp and the share of its plankton food. Polyps are not preserved in the fossil record, but the skeletal cups called corallites that make up the hard skeleton of corals are well preserved and are directly related to the size of the polyp. Corals with smaller corallites are usually more reliant on algae and thus are more efficient in photosymbiosis. In this study, we explored how the size of corallites relates to their ability to engage in photosymbiosis over the last ∼250 Myr. We used large datasets of fossil and modern corals and their corallite sizes. We applied various analytical methods to understand how photosymbiosis has evolved in reef-building corals. First, we analyzed the abundance or ecological dominance of different corallite sizes to understand ecological patterns. Second, we traced the diversity of corallite sizes over time in terms of taxonomic richness to identify evolutionary patterns. Our findings revealed interesting trends. When looking at corallite sizes by genus, we observed a slightly positive trend in corallite sizes in more recent times. However, when considering the ecological abundance of corallites, we found a significant negative trend in corallite sizes for colonial corals since the Mesozoic Era. This suggests that corals with smaller corallites became more dominant over time, thereby obtaining a competitive advantage in the shallow, tropical, nutrient-poor seas they largely occupy today.

## Abstract

Corallite sizes reflect a continuum in the efficacy of photosymbiosis in colonial reef corals, with smaller corallite sizes generally associated with higher autotrophy. Using a large compilation of reef-coral traits and corallite diameters as a proxy, we test here the hypothesis that photosymbiotic efficacy has increased over the evolutionary history of scleractinian corals. To gain a more comprehensive understanding of the evolutionary versus ecological patterns of corallite sizes of reef corals, we used three analytical methods: (1) occurrences-weighted within-bin analyses as a proxy for abundance or ecological dominance to depict ecological patterns; (2) unweighted range-through analyses; and (3) unweighted sampled-in-bin analyses to represent diversity in terms of taxonomic richness, enabling us to trace evolutionary patterns. By-genus, range-through analysis indicates a slightly positive trend of corallite sizes toward the Recent. However, the occurrences-weighted assessment shows a pronounced negative trend of corallite sizes in colonial corals since the Mesozoic. Random walk and directional evolution are both statistically supported to explain this long-term decrease. A driven trend is evolutionarily plausible, giving reef corals a selective advantage in the oligotrophic environments they largely occupy today.

## Introduction

Photosymbiosis—a mutually beneficial relationship between zooxanthellate algae and various groups of organisms—enables modern scleractinian corals to build reefs in nutrient-depleted settings (Perrin and Kiessling 2012). The breakdown of photosymbiosis in the context of coral bleaching has harmful consequences for the functioning of not just individual corals but of the entire reef ecosystems they build, which also endangers the survival of all reef-associated organisms (Hoegh-Guldberg et al. 2007; Hughes et al. 2017). The inferred presence or absence of photosymbionts in reef corals may also be linked to their evolutionary fate (Rosen 2000; Kiessling and Baron-Szabo 2004; Kiessling and Kocsis 2015; Stanley and van de Schootbrugge 2018). Photosymbiosis is seen as a prerequisite for the proliferation of coral reefs over time, including the Paleozoic (Coates and Jackson 1987; Zapalski et al. 2017; Bridge et al. 2022). Even the first well-preserved scleractinian corals from the Anisian Stage

(Middle Triassic, 246.7 Ma) adopted coloniality and are thought to have had a mutualistic relationship with symbiotic algae (i.e., zooxanthellae) as an adaptation for survival in a competitive reef environment (Kołodziej et al. 2018). However, photosymbiosis may not have been as efficient in those ancient corals as it is today. More specifically, early Mesozoic corals (Middle–Late Triassic) were suggested to have been symbiotically less efficient than their modern relatives (Nose and Leinfelder 1997).

Algal symbionts are not preserved in fossil coral skeletons; hence their presence has to be inferred using uniformitarian, morphological, or geochemical data. Given genetic constraints, the morphology of zooxanthellate corals (i.e., corals with zooxanthellae) should approach the most efficient light-harvesting strategy (Coates and Oliver 1973). Coral growth form, coloniality, corallite size, and colony integration have been proposed as morphological proxies for photosymbiosis (Coates and Jackson 1987; Kiessling and Baron-Szabo 2004; Zapalski et al. 2017). Morphological criteria perform well in predicting photosymbiosis in modern corals (Kiessling and Kocsis 2015), but only in a binary fashion distinguishing zooxanthellate and azooxanthellate corals (i.e., corals with and without zooxanthellae, respectively). However, there is a continuum in the efficacy of photosymbiosis in reef corals (Klaus et al. 2013; Radice et al. 2019; Sturaro et al. 2021). Among colonial corals, this continuum is reflected in corallite sizes (Conti-Jerpe et al. 2020). Smaller corallite sizes, and hence smaller polyp sizes, would increase the volume of surface area available for zooxanthellae, so they are better adapted to capture light and are therefore generally associated with higher photosymbiotic autotrophy. Corals with larger corallite (and polyp) sizes have low surface-to-volume ratios and are adapted to capture zooplankton; thus they are less dependent on photosymbionts (Porter 1976; Coates and Jackson 1987; Zapalski et al. 2017; Conti-Jerpe et al. 2020).

Here we investigate the long-term trends of corallite sizes in scleractinian corals from the Middle Triassic (246.7 Ma) to the Holocene (0.0117 Ma) testing the hypothesis that there was an increase in photosymbiotic efficacy over the evolutionary history of scleractinian corals. We combine fossil occurrence data from the Paleobiology Database (PBDB) with morphological traits from the Ancient Reef Traits Database (ARTD) and the Coral Traits Database (CTD). As a proxy for ecological trends, we used occurrences-weighted mean corallite sizes and as a proxy for evolutionary trends we referred to unweighted range-through and sampled-in-bin means. We expected that ecological and evolutionary trends would show a good match, exhibiting similar macroevolutionary patterns, as previous studies have shown (Aberhan et al. 2006; Madin et al. 2006).

## Methods

### Data

Data on corallite sizes were obtained from the ARTD (https://art.nat.fau.de) (Raja et al. 2022), which contains trait information of various reef-building organisms from published and unpublished resources. The database as of June 2022 contains 3322 measurements of corallite diameters for 406 genera of fossil scleractinian corals (Supplementary Fig. 1). Corallite data of extant corals (94 genera) were obtained from the CTD (Madin et al. 2016). Fossil occurrence data were extracted from PBDB (https://paleobiodb.org) using the chronosphere package (v. 0.4.0) (Kocsis and Raja 2020) for R (v. 4.1.2) on February 20, 2022. The PBDB dataset consisted of 31,579 occurrences of 802 scleractinian genera. The
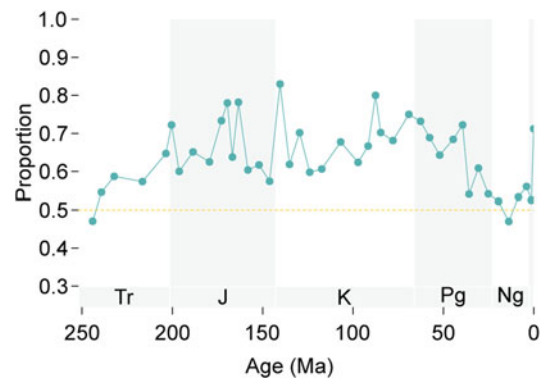


**Figure 1.** Proportion of colonial scleractinian genera containing measurement of corallite diameter relative to all colonial scleractinian genera from the Paleobiology Database in each geological stage (marked with points). Tr, Triassic; J, Jurassic; K, Cretaceous; Pg, Paleogene; Ng, Neogene.

proportion of scleractinian genera containing corallite diameter measurement relative to all scleractinian genera from the PBDB was on average 64%, with little temporal variation through time (Fig. 1).

Analyses were performed at the genus level, because this is the most reliable level of taxonomic classification of fossil corals (Lathuiliere 1996; Fig. 2). Taxa with uncertain genus identification were excluded, as were occurrences that could not be assigned to a single geological stage. Data were binned to stages and the time-scale of Gradstein et al. (2020), spanning from the Middle Triassic (Anisian Stage, 246.7 Ma) to the Holocene (Supplementary Table 1). Because some data in the ARTD and the CTD contain specimen-level corallite size ranges (i.e., minimum and maximum values), we first calculated the mean corallite widths for the specimens containing these corallite size ranges for each dataset. Due to the scarcity of specimen-based data, we treated corallite diameter as fixed through the duration of a genus. To test within-genus variation, we chose eight representative genera with ranges spanning longer than 20 Myr that contain three or more species with at least two specimens (*Calamophylliopsis*, *Ceriostella*, *Cladophyllia*, *Isastrea*, *Microsolena*, *Retiophyllia*, *Stylosmilia*, and *Thecosmilia*). We found no trend over time for any of these genera, which supports the use of static genus corallite sizes (Supplementary Fig. 2A–H).

### Data Analysis Protocol

We first computed the mean corallite sizes of species for each of the datasets, whereby we excluded the unknown species. The mean species' values from ARTD and CTD were combined to compute the mean corallite size of genera. These values were then assigned to fossil occurrences in the PBDB to depict ecological patterns (i.e., weighted by the occurrences) (Fig. 2). To track changes over time, the mean corallite sizes of genera were assessed in two ways: (1) according to the inferred range-through presence of genera in a time bin and (2) sampled-in-bin genera (Fig. 2). The final dataset of PBDB occurrences comprised 27,173 measurements of corallite diameter for 291 fossil and Recent coral genera. Subsequently, the dataset was split into colonial (excluding free-living, i.e., not attached, and known modern azooxanthellate corals, $n = 225$) and solitary ($n = 62$) corals, and the mean corallite width was calculated for each stage (Fig. 2). In addition to means, we also calculated the median corallite width for each
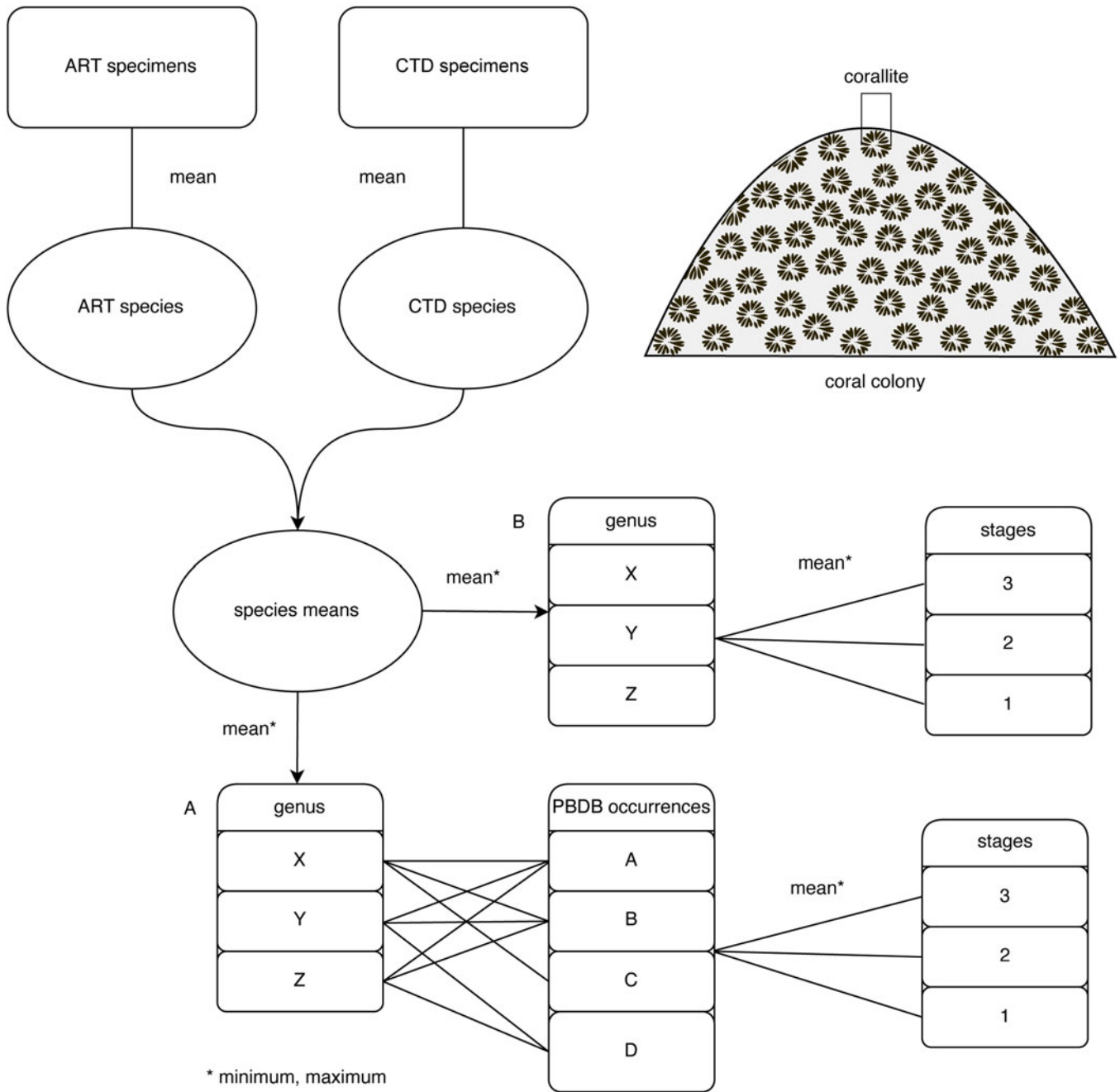
**Figure 2.** Data analysis protocol for: A, occurrences-weighted analyses; and B, unweighted diversity-based analyses. ART, Ancient Reef Traits Database; CTD, Coral Traits Database; PBDB, Paleobiology Database.

stage to check whether the use of medians affects the basic results. We followed the same protocol for calculating the minimum and maximum corallite sizes per geological stage. The minimum and maximum values of genera were calculated from the pool of species' means, whereby each genus was assigned the smallest and largest species' mean values, respectively. The minimum and maximum values of genera were then calculated for each stage, respectively (Fig. 2).

## Trend Analyses

To obtain a more comprehensive understanding of the underlying drivers, we used three analytical methods to derive trends:

1. Occurrences-weighted within-bin analyses: We assigned corallite sizes to all occurrences of coral genera, which served as a proxy for abundance or ecological dominance to depict ecological patterns.
2. Unweighted range-through analyses: We assigned corallite sizes to the inferred range-through presence of genera in time bins. This allowed us to represent diversity in terms of taxonomic richness, enabling us to depict evolutionary patterns.
3. Unweighted sampled-in-bin analyses: We assigned corallite sizes based on a recorded presence of genera in a given time bin. This represents taxonomic richness, aiding in the depiction of evolutionary patterns.

We applied generalized additive models (GAMs) to investigate the long-term trend of corallite sizes over time. GAMs are useful for modeling nonlinear data and provide a more effective tool to model complex phenomena than do traditional linear models (Ravindra et al. 2019). We applied GAM curve fitting with the 95% confidence interval for the mean shape of the effect using the mgcv package with the default settings (v. 1.8.31) (Wood 2017) to model the nonlinear relationships of corallite width through time. Smooth terms are represented using penalized regression splines, with smoothing parameters selected by the restricted maximum likelihood method. In addition to GAMs, we also fit a linear model estimate to assess the overall trend of mean and median corallite sizes over time.

The existence of a trend in corallite sizes through time was also statistically tested with the paleoTS package (v. 0.5.2) (Hunt 2006). The parameters used to estimate the models are the mean value of the trait (here, corallite width) and the variance of the mean corallite widths of genera for each stage, sample size, and age. This method evaluates the maximum likelihood of three models: directional trend or generalized random walk (GRW), unbiased random walk (URW), and stasis. The GRW model is determined by mean and variance, wherein the mean governs the directionality of the trend and variance determines the volatility of evolutionary changes around the directional trend (Hunt 2006). For the URW model, the mean equals zero, and the trend is considered nondirectional. The stasis model assumes a certain variation of a fixed mean and no trend over time. The best-fit model was estimated based on the corrected Akaike information criteria (AICc) (Hunt 2006). However, if the difference in the AICc scores between the models was small (<2 units), then these models were not considered significantly less credible than the best-fit model (Burnham and Anderson 2003).

To further assess model adequacy, we used the package adePEM (v. 1.1) (Voje 2018). This package tests the GRW and URW models for autocorrelation, length of runs, and fixed variance, and the stasis model for an additional net change test over time. It uses the parameters of the fitted models and checks whether they are likely to belong to the same distribution. The number of bootstrap replications used for assessing model adequacy was set at 10,000 and the confidence level at 0.95. The best-fit model was rendered adequate if it passed all three tests.

To test the correspondence between ecological and evolutionary patterns, we performed cross-correlation analyses between (1) occurrences-weighted and unweighted range-through, (2) occurrences-weighted and unweighted sampled-in-bin, and (3) unweighted range-through and unweighted sampled-in-bin mean corallite sizes.

## Results

### Colonial Corals
*Occurrences-weighted Analyses.* We observed an overall decrease of mean corallite sizes from the Middle Triassic until the Recent, which appears to have two phases: one from the Middle Triassic (246.7 Ma) and a second across the entire Cenozoic (Fig. 3A). The overall linear regression model was: corallite width $= 4.48 - 0.0098 *$ age (adjusted $R^2 = 0.14$, $p = 0.008$). We observed a decrease in median corallite sizes: corallite width $= 1.84 - 0.02 *$ age (adjusted $R^2 = 0.6$, $p < 0.001$) (Fig. 4A).



**Figure 3.** Trajectories of mean corallite width (mm) of colonial scleractinian coral genera over time for: A, occurrences-weighted, B, unweighted diversity-based range-through, and C, unweighted diversity-based sampled-in-bin. The trend line (in yellow) is the fitted line from the generalized additive model. The dashed gray line is the linear regression line. The shaded area represents 95% confidence intervals. The bars represent the standard errors of individual estimates. Tr, Triassic; J, Jurassic; K, Cretaceous; Pg, Paleogene; Ng, Neogene.

The minimum corallite width decreased over time, while the maximum increased until the Early Cretaceous, after which it remained stable (Fig. 5). This is particularly noticeable on the graph of stratigraphic ranges of genera against their corallite sizes (Supplementary Fig. 3). This pattern is expected in a diffusion process (URW). Statistical tests for the three basic models of evolutionary trends (GRW, URW, and stasis) (Hunt 2006),
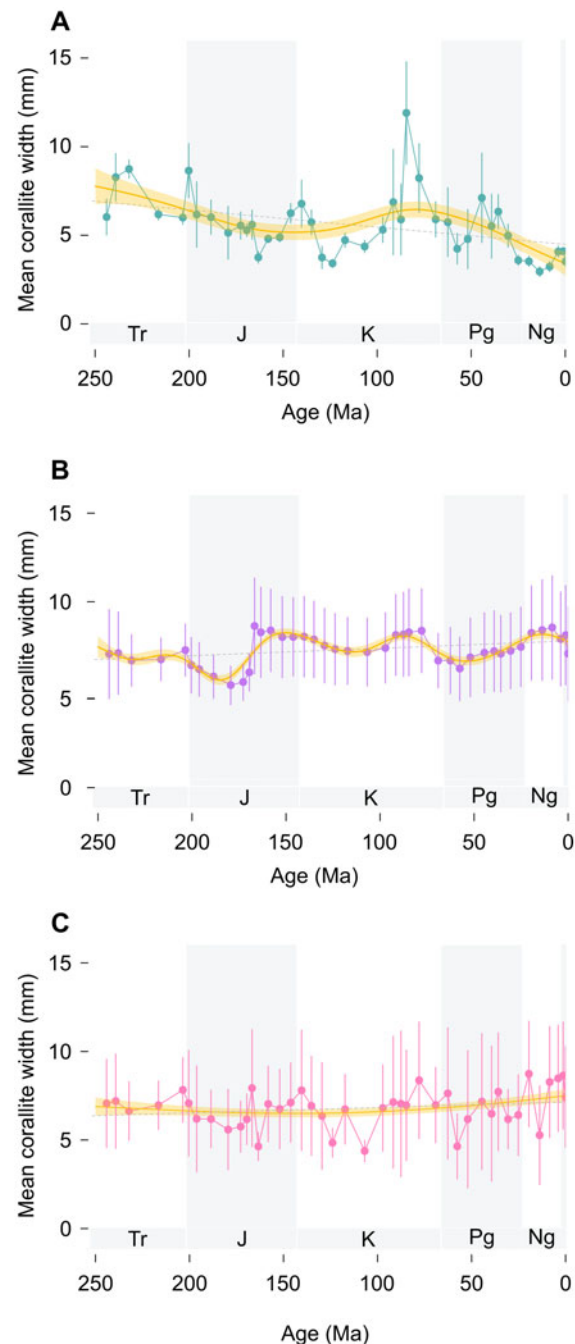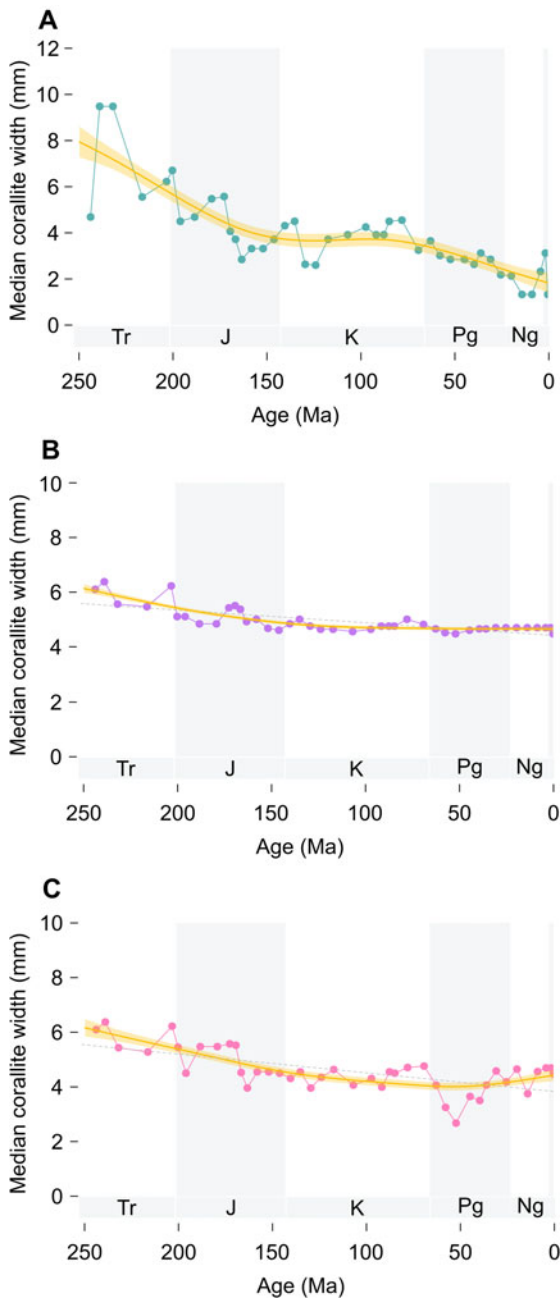
**Figure 4.** Trajectories of median corallite width (mm) of colonial scleractinian coral genera over time for: A, occurrences-weighted, B, unweighted diversity-based range-through, and C, unweighted diversity-based sampled-in-bin. The trend line (in yellow) is the fitted line from the generalized additive model. The shaded area represents 95% confidence intervals. The dashed gray line is the linear regression line; (Tr, Triassic; J, Jurassic; K, Cretaceous; Pg, Paleogene; Ng, Neogene).

supported that URW is indeed the best-fit model (Table 1, Supplementary Figs. 4–6). However, we could not reject the GRW (Supplementary Fig. 4), because the ΔAICc value for this model is lower than the critical value of 2 units relative to the URW model (Table 1). Furthermore, both models passed all three adequacy tests (i.e., autocorrelation, runs, and fixed variance) (Table 2, Fig. 6, Supplementary Fig. 7).

To observe evolutionary patterns that emerge within clades, we selected five colonial families with more than 1000 fossil occurrences: Acroporidae, Latomeandridae, Merulinidae, Poritidae,

and Stylinidae. Two families with the largest number of occurrences—Acroporidae and Poritidae—decreased in corallite sizes over time (Fig. 7A,D). Contrary to the long-term decrease in corallite sizes of all colonial corals, the Merulinidae increased in corallite sizes, while there was no trend in the Stylinidae and Latomeandridae (Fig. 7B,C,E). The statistical outputs of evolutionary trend models varied across and within clades (Supplementary Table 2). For example, the best-fit model for the Acroporidae family was URW, but GRW passed all three adequacy tests. The GRW also passed all adequacy tests for Merulinidae, Poritidae, and Stylinidae families (Supplementary Table 2). However, in addition to the GRW model, Poritidae and Stylinidae also passed the URW model, while Merulinidae passed the stasis model. Adequacy tests showed that URW and stasis were best-fit models for the family Latomeandridae (Supplementary Table 2).

*Range-through Analyses.* We found a slightly positive trend for the unweighted diversity-based range-through genus means (Fig. 3B). The fitted regression model was: corallite width = 7.8 + 0.004 * age (adjusted $R^2 = 0.1$, $p = 0.02$). Because the family Mussidae has unusually large corallite sizes for colonial corals (~60 mm), we checked whether the overall trend is driven by this single family. Indeed, there was no trend after the removal of the family Mussidae (Supplementary Fig. 8). The fitted regression model was: corallite width = 6.6 + 0.002 * age (adjusted $R^2 = 0.01$, $p = 0.2$). Using medians instead of means provided the same basic trend, albeit with a better fit: corallite width = 4.4 + 0.004 * age (adjusted $R^2 = 0.5$, $p < 0.001$) (Fig. 4B).

As in the occurrences-weighted analysis, the minimum corallite width of all range-through genera decreased, while the maximum increased (Supplementary Figs. 9, 10). Statistical tests for the three basic models of evolutionary trends of all range-through genera support stasis as the best-fit model (Table 1, Supplementary Figs. 11–13). However, neither of these models passed the adequacy tests (Table 2, Supplementary Figs. 14–16).

*Sampled-in-Bin Analyses.* We found no significant trend for the unweighted diversity-based sampled-in-bin analyses using means (adjusted $R^2 = 0.02$, $p = 0.2$) (Fig. 3C). However, the median corallite width decreased slightly over time: corallite width = 3.8 + 0.01 * age (adjusted $R^2 = 0.4$, $p < 0.001$) (Fig. 4C). The minimum corallite width decreased, while the maximum increased over time (Supplementary Figs. 17, 18).

While statistical tests support GRW as the best-fit model (Table 1, Supplementary Figs. 19–21), all three models passed all adequacy tests (Table 2, Supplementary Figs. 22–24).

*Cross-correlation.* We performed cross-correlation analyses to test the correspondence between ecological and evolutionary trends. We found a weak negative cross-correlation between occurrences-weighted and range-through mean corallite sizes, and a weak positive cross-correlation between occurrences-weighted and sampled-in-bin mean corallite sizes (Table 3). A strong positive correlation existed between range-through and sampled-in-bin mean corallite sizes (Table 3).

## Solitary Corals

The occurrences-weighted mean corallite width of solitary corals was stable until the Neogene, when it drastically increased, until the Recent (adjusted $R^2 = 0.003$, $p = 0.3$) (Fig. 8A). The increase
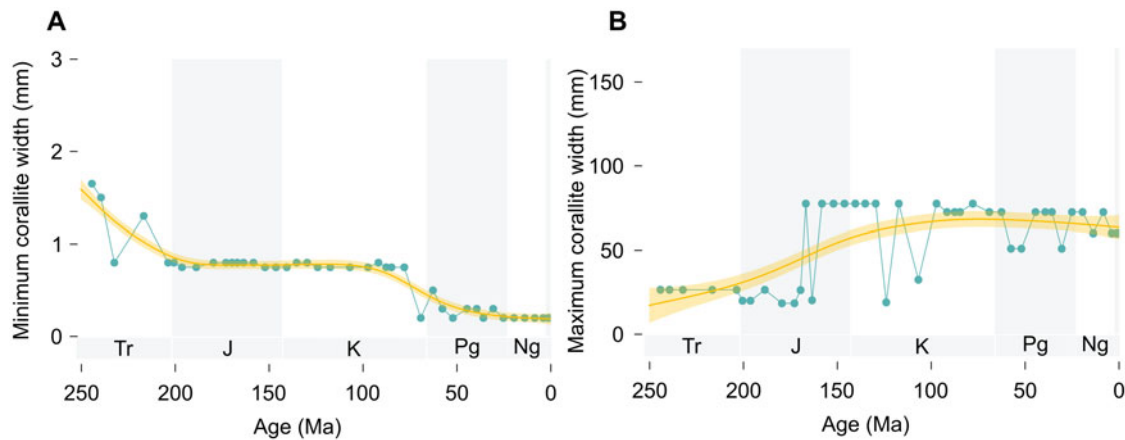
**Figure 5.** Trajectories of minimum (A) and maximum (B) corallite width (mm) of colonial scleractinian genera occurrences over time. The trend line (in yellow) is the fitted line from the generalized additive model. The shaded area represents 95% confidence intervals. The points mark minimum and maximum corallite sizes in each stage. Tr, Triassic; J, Jurassic; K, Cretaceous; Pg, Paleogene; Ng, Neogene.

is mostly driven by the family Fungiidae, but still significant when this family is excluded (adjusted $R^2 = 0.1$, $p = 0.03$).

Similar to colonial corals, the minimum of all solitary corals decreased, while the maximum increased over time (Supplementary Figs. 25, 26). The best-fit model for solitary corals was again the URW, but similar to the colonial corals, ΔAICc for the GRW was less than 2 units relative to the URW model (Table 1, Supplementary Figs. 27–29). However, when adequacy tests were performed, the URW model failed the autocorrelation and fixed variance tests, rendering a GRW—which passed all three tests—the best model (Table 2, Supplementary Figs. 30–32).

## Discussion

Our study provides the first assessment of trends in corallite sizes over geological time. Surprisingly, we found opposing long-term

trends depending on the analytical protocol. This is reminiscent of a previous study showing that there was a decoupling of evolutionary success and ecological dominance in bryozoans across the Cretaceous/Paleogene boundary (McKinney et al 1998). The occurrences-weighted pattern (reflecting the dominance of ecological groups) signified a long-term trend toward smaller corallite sizes, whereas the unweighted diversity-based estimators showed a slightly increasing trend (Fig. 3). We observed the same mismatch for the median corallite widths (Fig. 4). In this sense, our study provides a case study when richness-based and dominance-based patterns do not match over long timescales. Previous assessments demonstrated a good match between the two patterns (Aberhan et al. 2006; Madin et al. 2006). However, these authors only used sampled-in-bin estimates for both richness and ecological dominance. The discrepancy in our dataset is largely between occurrences-weighted versus range-through, but also between occurrences-weighted and sampled-in-bin.

**Table 1.** Model fit estimates of the analyzed time series for occurrences-weighted, and unweighted range-through and sampled-in-bin colonial and solitary scleractinian corals. Models used are GRW (generalized random walk or directional change), URW (unbiased random walk), and stasis. Estimates of the best model(s) are marked in bold. AICc, Akaike information criteria; ΔAICc, the difference between the AICc and the minimum AICc.

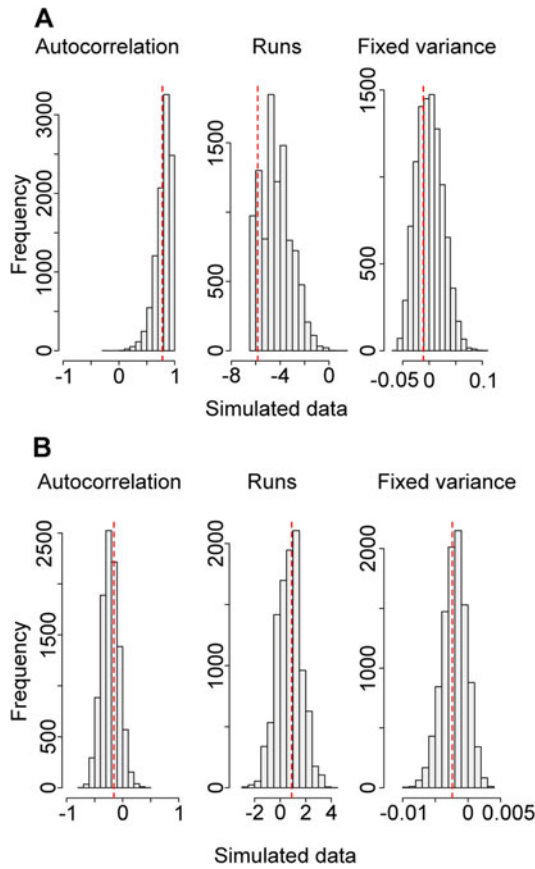| Model | Colonial | | | Solitary | | |
|---|---|---|---|---|---|---|
| | AICc | ΔAICc | Weight | AICc | ΔAICc | Weight |
| Occurrence-weighted | | | | | | |
| GRW | 161.4 | **2** | 0.3 | 349 | **1.6** | 0.3 |
| URW | 159.4 | **0** | 0.7 | 347.4 | **0** | 0.7 |
| Stasis | 167.5 | 8.1 | 0.01 | 357.7 | 10.3 | 0.004 |
| Range-through | | | | | | |
| GRW | 115.4 | **1.6** | 0.2 | 295.2 | **1.5** | 0.3 |
| URW | 113.9 | **0** | 0.4 | 293.7 | **0** | 0.7 |
| Stasis | 113.9 | **0** | 0.4 | 331.5 | 37.8 | 0 |
| Sampled-in-bin | | | | | | |
| GRW | 128.7 | **0** | 0.4 | 299.1 | **1.4** | 0.3 |
| URW | 129 | **0.4** | 0.3 | 297.7 | **0** | 0.7 |
| Stasis | 129 | **0.4** | 0.3 | 324.6 | 26.8 | 0 |

**Figure 6.** Distribution of adequacy tests autocorrelation, length of runs, and fixed variance for occurrences-weighted colonial scleractinian corals using 10,000 simulated data sets: A, the directional change model (GRW); and B, the random walk model (URW). The red dashed vertical lines indicate the values of the test statistic from the observed data.

Notably, we have not found a cross-correlation between the richness-based and dominance-based patterns (Table 3). Occurrences-weighted analyses have not been performed for the reported ecological trends in predation, motility, and physiological buffering (e.g., Bambach et al. 2002). This opens up possibilities for further investigation of the robustness of the Phanerozoic-scale ecological trends that were primarily derived from richness-based range-through analyses reported in such studies.

### Potential Biases

Sampling biases plague all kinds of paleontological analyses. This includes patterns over time (e.g., Alroy et al. 2001) and space (e.g., Vilhena and Smith 2013; Close et al. 2020). In ignoring variations of sampling and giving equal weight to abundant and rare taxa, range-through estimates may arguably be most affected by sampling biases. Occurrences-weighted analyses reflect the rank order of abundances and give more weight to abundant taxa (e.g., Alroy et al. 2001). The occurrences-weighted analyses could be prone to spatial biases (Benson et al. 2021; Flannery-Sutherland et al. 2022). However, the paleolatitudinal distribution of our occurrences shows that there was modest variation in latitudinal sampling, which is centered in the subtropics throughout (Supplementary Fig. 33). Sampling of reef corals usually follows reef distribution, which was always limited to tropics and subtropics. Indeed, 80% of colonial corals in our dataset come from the reefs. Therefore, occurrences-weighted analyses are preferable to explore long-term paleontological trends, and these have been applied in previous studies on morphological trends (e.g., Hunt 2007).

Our occurrences-weighted long-term trend indicates that smaller corallites became more prevalent over time. This is
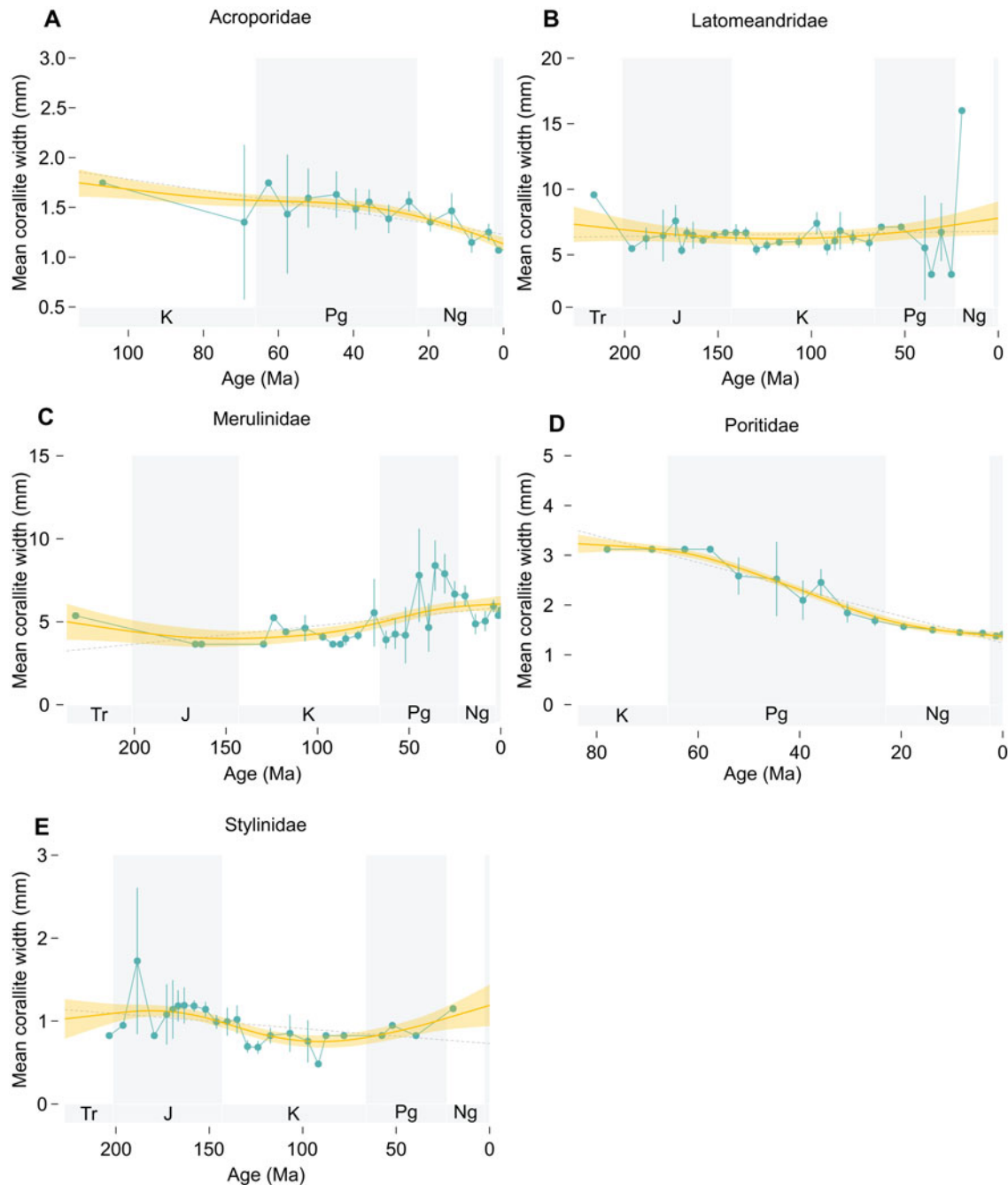
**Table 2.** Results of the adequacy tests (autocorrelation, runs, and fixed variance) for the two analyzed models of change in corallite size: GRW (generalized random walk or directional change) and URW (unbiased random walk) and an additional net-change test for the stasis model for occurrences-weighted, and unweighted range-through and sampled-in-bin colonial and solitary scleractinian corals. *p*-values greater than 0.05, marked in bold, indicate that the specific test was passed (Voje 2018).

| Adequacy tests | Colonial | | | Solitary | | |
| --- | --- | --- | --- | --- | --- | --- |
| | GRW | URW | Stasis | GRW | URW | Stasis |
| Occurrence-weighted | | | | | | |
| Autocorrelation | **0.1** | **0.4** | 0 | **0.9** | <0.001 | 0 |
| Runs | **0.3** | **0.7** | 0.002 | **0.3** | **0.4** | 0.05 |
| Fixed variance | **0.9** | **0.5** | **0.4** | **0.5** | 0 | 0 |
| Net change | NA | NA | **0.1** | NA | NA | 0 |
| Range-through | | | | | | |
| Autocorrelation | 0 | <0.001 | 0 | **0.5** | 0 | 0 |
| Runs | 0 | 0.005 | 0 | **0.1** | 0 | 0 |
| Fixed variance | **0.7** | **0.6** | **0.7** | **0.3** | 0 | 0 |
| Net change | NA | NA | **1** | NA | NA | <0.001 |
| Sampled-in-bin | | | | | | |
| Autocorrelation | **0.8** | **0.3** | **0.8** | **0.2** | 0.001 | 0 |
| Runs | **0.6** | **0.6** | **0.3** | **0.05** | **0.4** | 0.02 |
| Fixed variance | **0.8** | **0.2** | **0.1** | **0.5** | 0 | 0 |
| Net change | NA | NA | **0.8** | NA | NA | <0.001 |

**Figure 7.** Trajectories of mean corallite width (mm) of common (occurrences-weighted) colonial scleractinian families over time: A, Acroporidae; B, Latomeandridae; C, Merulinidae; D, Poritidae; and E, Stylinidae. The trend line (in yellow) is the fitted line from the generalized additive model. The points mark mean corallite sizes in each stage. The dashed gray line is the linear regression line. The blue bars represent the standard errors. Tr, Triassic; J, Jurassic; K, Cretaceous; Pg, Paleogene; Ng, Neogene.

**Table 3.** Results of cross-correlation (R) between occurrences-weighted and unweighted diversity-based corallite sizes at lag zero for colonial scleractinian genera.

| Cross-correlation | R |
|---|---|
| Range-through and occurrences-weighted | −0.10 |
| Sampled-in-bin and occurrences-weighted | 0.22 |
| Range-through and sampled-in-bin | 0.41 |

particularly obvious in the two most abundant clades—Acroporidae and Poritidae (Fig. 7A,D). Due to their abundance, the two families are likely responsible for the overall Cenozoic decline in corallite sizes. Similarly, the unweighted range-through trend is also potentially influenced by a single family. Despite an overall positive trend, the exclusion of the family Mussidae revealed the absence of any trend (Supplementary Fig. 8). Also, solitary corals increased in corallum size from the Neogene onward, and this increase is entirely due to the radiation of one single clade, the Fungiidae, which are the zooxanthellate family
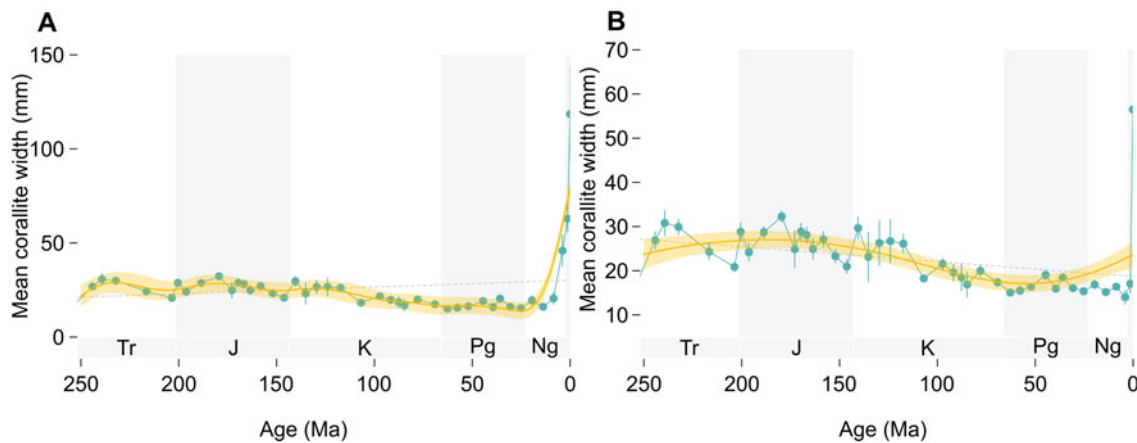
**Figure 8.** Trajectories of mean corallite width (mm) of occurrences-weighted solitary scleractinian genera: A, all occurrences; and B, occurrences without family Fungiidae over time. The trend line (in yellow) is the fitted line from the generalized additive model. The dashed gray line is the linear regression line. The blue bars represent the standard errors. Tr, Triassic; J, Jurassic; K, Cretaceous; Pg, Paleogene; Ng, Neogene.

(Fig. 8B). These observations and the absence of a significant trend in the diversity-based sampled-in-bin analyses suggest that the occurrences-weighted analyses are the most robust for depicting biologically meaningful long-term trends.

### Directionality versus Random Walk

We found that both URW and GRW are plausible for occurrences-weighted and unweighted sampled-in-bin analyses, while range-through analyses indicate stasis. Long-term evolutionary trends can be passive (i.e., URW) or driven (i.e., GRW) (McShea 1994). In a driven system, a driver determines the direction of a change (McShea 1994). A passive trend is usually governed by some constraint boundary (McShea 1994). For example, in the context of body sizes, there is usually a lower boundary, because there is a minimum size for metazoan life and increases in sizes must therefore be more common than decreases (e.g., Cope's rule; Heim et al. 2015; Payne and Heim 2020). In the case of corallite sizes, such a boundary effect is not noticeable. On the contrary, the greater range of corallite sizes over time would support a diffusion model (i.e., URW). Regarding body sizes, a driven trend can most easily be detected when both the minimum and the maximum evolve in the same direction, even though the patterns of minimum and maximum should not always be detrimental to the directionality of the evolutionary trends (McShea 1994, 1998). For the occurrences-weighted analyses, we show that the maximum corallite sizes of colonial corals remained stable from the Early Cretaceous onward, while the minimum values decreased over time, which is suggestive of a simple diffusion (i.e., URW) as the underlying process (Fig. 5). This diffusion model is also supported by statistical tests (Table 1). However, the statistical method (Hunt 2006) might be biased toward the URW. The URW can likely generate a wide range of trait dynamics compared with other models, but this does not imply that the majority of lineages evolve according to URW (Voje 2018). However, both URW and GRW models passed the adequacy tests for occurrences-weighted analyses (Table 2). This aligns well with the observation that adequacy tests are not always detrimental to a particular model (Voje 2018). The family-level analyses also provided ambiguous best-fit model results (Supplementary Table 2). This again indicates that both URW and GRW are plausible for occurrences-weighted analyses, but

neither is conclusive. Given the further equivocal outcomes of the best-fit model results obtained from the unweighted range-through and sampled-in-bin analyses, the case must remain unresolved in a statistical sense. However, we argue that a biological underpinning of the observed ecological trend is likely.

### Photosymbiosis over Time

The decreasing trend of corallite sizes in the early Mesozoic for occurrences-weighted analyses (Fig. 3A) may indicate an increasing reliance of corals on photosymbiosis. Previous work suggested that early corals already achieved photosymbiosis (Stanley and Swart 1995; Zapalski et al. 2017; Bridge et al. 2022) but may have relied less on photosynthetic algae than modern corals (Nose and Leinfelder 1997; Leinfelder 2001; Stanley 2003). Morphological characters indicative of photosymbiosis (coloniality, small corallite sizes, high colony integration, etc.) and isotopic analyses (Stanley and Swart 1995) indicated that photosymbiosis already evolved in the Middle Triassic and became widespread by the Late Triassic (Stanley 2003; Stanley and Helmle 2010; Kołodziej et al. 2018). Observations of reduced low- to high-density growth band ratios were taken as evidence for a greater share of heterotrophic feeding in Late Jurassic reef corals than in modern corals (Nose and Leinfelder 1997). Nose and Leinfelder (1997) argued that Jurassic corals did not have a fully developed symbiotic relationship and were probably able to switch between zooxanthellate and azooxanthellate states because they were not yet perfectly adapted to oligotrophic settings but also grew in mesotrophic environments with high siliciclastic input. However, there is limited evidence that Jurassic corals thrived in more turbid environments than modern corals. The distribution of reefs in siliciclastic settings was also high in the Neogene (Kiessling 2002), and this was a time of increased reef development and coral diversification. Corallite integration—the way corallites are arranged in colonial corals—has also increased since the Triassic (Coates and Oliver 1973; Coates and Jackson 1987), which also supports higher evolutionary reliance on photosymbionts through time (Coates and Oliver 1973; Coates and Jackson 1987; Stanley and van de Schootbrugge 2018).

Corallite sizes of colonial corals decreased over the period of nearly 250 Myr. Even though it remains unclear whether this decrease is a driven trend or a random walk, it shows that larger

corallite corals became less common over time and that colonial corals overall improved their photosymbiotic efficacy. Unfortunately, this adaptation has led modern corals into an evolutionary predicament: their reliance on photosymbionts renders corals particularly vulnerable to climate change (Hughes et al. 2017).

## Literature Cited

Aberhan, M., W. Kiessling, and F. T. Fürsich. 2006. Testing the role of biological interactions in the evolution of mid-Mesozoic marine benthic systems. *Paleobiology* 32:259–277.

Alroy, J., C. R. Marshall, R. K. Bambach, K. Bezusko, M. Foote, F. T. Fürsich, T. A. Hansen, *et al.* 2001. Effects of sampling standardization on estimates of Phanerozoic marine diversification. *Proceedings of the National Academy of Sciences USA* 98:6261–6266.

Bambach, R. K., A. H. Knoll, and J. J. Sepkoski Jr. 2002. Anatomical and ecological constraints on Phanerozoic animal diversity in the marine realm. *Proceedings of the National Academy of Sciences USA* 99:6854–6859.

Benson, R. B. J., R. Butler, R. A. Close, E. E. Saupe, and D. L. Rabosky. 2021. Biodiversity across space and time in the fossil record. *Current Biology* 31:R1225–R1236.

Bridge, T. C. L., A. H. Baird, J. M. Pandolfi, M. J. McWilliam, and M. K. Zapalski. 2022. Functional consequences of Palaeozoic reef collapse. *Scientific Reports* 12:1386

Burnham, K. P., and D. R. Anderson. 2003. *Model selection and multimodel inference: a practical information-theoretic approach.* Springer, New York.

Close, R. A., R. B. J. Benson, E. E. Saupe, M. E. Clapham, and R. J. Butler. 2020. The spatial structure of Phanerozoic marine animal diversity. *Science* 368:420–424.

Coates, A. G., and J. B. C. Jackson. 1987. Clonal growth, algal symbiosis, and reef formation by corals. *Paleobiology* 13:363–378.

Coates, A. G., and W. A. Oliver. 1973. Coloniality in Zoantharian corals. Pp. 3–27 in R. S. Boardman, A. Cheetam, and W. A. J. Oliver, eds. *Animal colonies—development and function through time.* Dowden, Hutchinson & Ross, Stroudsburg.

Conti-Jerpe, I. E., P. D. Thompson, C. W. M. Wong, N. L. Oliveira, N. N. Duprey, M. A. Moynihan, and D. M. Baker. 2020. Trophic strategy and bleaching resistance in reef-building corals. *Scientific Advances* 6: eaaz5443.

Flannery-Sutherland, J. T., D. Silvestro, and M. J. Benton. 2022. Global diversity dynamics in the fossil record are regionally heterogeneous. *Nature Communications* 13:2751.

Gradstein, F. M., and J. G. Ogg. 2020. The Chronostratigraphic Scale. Pp. 21–32 in *Geologic Time Scale 2020.* Elsevier, Amsterdam.

Heim, N. A., M. L. Knope, E. S. Schaal, S. C. Wang, and J. L. Payne. 2015. Cope's rule in the evolution of marine animals. *Science* 347:867–870.

Hoegh-Guldberg, O., P. J. Mumby, A. J. Hooten, R. S. Steneck, P. Greenfield, E. Gomez, C. D. Harvell, *et al.* 2007. Coral reefs under rapid climate change and ocean acidification. *Science* 318:1737–1742.

Hughes, T. P., J. T. Kerry, M. Alvarez-Noriega, J. G. Alvarez-Romero, K. D. Anderson, A. H. Baird, R. C. Babcock, *et al.* 2017. Global warming and recurrent mass bleaching of corals. *Nature* 543:373–377.

Hunt, G. 2006. Fitting and comparing models of phyletic evolution: random walks and beyond. *Paleobiology* 32:578–601.

Hunt, G. 2007. The relative importance of directional change, random walks, and stasis in the evolution of fossil lineages. *Proceedings of the National Academy of Sciences USA* 104:18404–18408.

Kiessling, W. 2002. Secular variations in the Phanerozoic reef ecosystem. *In* W. Kiessling, E. Flügel, and J. Golonka, eds. *Phanerozoic reef patterns.* SEPM Special Publication 72:625–690. Society for Sedimentary Geology, Tulsa, Okla.

Kiessling, W., and R. C. Baron-Szabo. 2004. Extinction and recovery patterns of scleractinian corals at the Cretaceous–Tertiary boundary. *Palaeogeography, Palaeoclimatology, Palaeoecology* 214:195–223.

Kiessling, W., and Á. T. Kocsis. 2015. Biodiversity dynamics and environmental occupancy of fossil azooxanthellate and zooxanthellate scleractinian corals. *Paleobiology* 41:402–414.

Klaus, J. S., S. T. Murray, P. K. Swart, and D. F. McNeill. 2013. Resource partitioning and paleoecology of Neogene free-living corals as determined from skeletal stable isotope composition. *Bulletin of Marine Science* 89:937–954.

Kocsis, Á. T., and N. B. Raja. 2020. Chronosphere: Earth system history variables. https://doi.org/10.5281/zenodo.3525482.

Kołodziej, B., K. Salamon, E. Morycowa, J. Szulc, and M. A. Łabaj. 2018. Platy corals from the Middle Triassic of Upper Silesia, Poland: implications for photosymbiosis in the first scleractinians. *Palaeogeography, Palaeoclimatology, Palaeoecology* 490:533–545.

Lathuiliere, B. 1996. Is morphology a good way to understand the evolution of corals? *Paleontological Society Papers* 1:81–105.

Leinfelder, R. 2001. Jurassic reef ecosystems. Pp. 251–309 in G. D. Stanley, ed. *The history and sedimentology of ancient reef systems.* Plenum Press, New York.

Madin J. S., J. J. Alroy, M. Aberhan, F. T. Fürsich, W. Kiessling, M. A. Kosnik, and P. J. Wagner. 2006. Statistical independence of escalatory ecological trends in Phanerozoic marine invertebrates. *Science* 312:897–900.

Madin, J. S., K. D. Anderson, M. H. Andreasen, T. C. Bridge, S. D. Cairns, S. R. Connolly, E. S. Darling, *et al.* 2016. The Coral Trait Database, a curated database of trait information for coral species from the global oceans. *Scientific Data* 3:160017.

McKinney, F. M., S. Lidgard, J. J. Sepkoski Jr., and P. D. Taylor. 1998. Decoupled temporal patterns of evolution and ecology in two post-Paleozoic clades. *Science* 281:807–809.

McShea, D. W. 1994. Mechanisms of large-scale evolutionary trends. *Evolution* 48:1747–1763.

McShea, D.W. 1998. Possible largest-scale trends in organismal evolution: eight "live hypotheses." *Annual Review of Ecology, Evolution, and Systematics* 29:293–318.

Nose, W., and R. R. Leinfelder. 1997. Upper Jurassic coral communities within siliciclastic settings (Lusitanian Basin, Portugal), implications for symbiotic and nutrient strategies. Pp. 1755–1760 in *Proceedings of the 8th International Coral Reef Symposium, Panama.*

Payne J. L., and N. A. Heim. 2020. Body size, sampling completeness, and extinction risk in the marine fossil record. *Paleobiology* 46:23–40.

Perrin, C., and W. Kiessling. 2012. Latitiudinal trends in Cenozoic reef patterns and their relationship to climate. Pp. 17–33 in *Carbonate systems during the Oligocene–Miocene climatic transition.* Wiley, Hoboken, N.J.

Porter, J. W. 1976. Autotrophy, heterotrophy, and resource partitioning in Caribbean reef-building corals. *American Naturalist* 110:731–742.

Radice, V. Z., O. Hoegh-Guldberg, B. Fry, M. D. Fox, S. G. Dove, and E. Dorrepaal. 2019. Upwelling as the major source of nitrogen for shallow and deep reef-building corals across an oceanic atoll system. *Functional Ecology* 33:1120–1134.

Raja, N. B., D. Dimitrijević, M. C. Krause, and W. Kiessling. 2022. Ancient Reef Traits, a database of trait information for reef-building organisms over the Phanerozoic. *Scientific Data* 9:425.

Ravindra, K., P. Rattan, S. Mor, and A. N. Aggarwal. 2019. Generalized additive models: building evidence of air pollution, climate change and human health. *Environment International* **132**:104987.

Rosen, B. R. 2000. Algal symbiosis, and the collapse and recovery of reef communities: Lazarus corals across the K-T boundary. Pp. 164–180 *in* S. J. Culver and P. F. Rawson, eds. *Biotic response to global change: the last 145 million years*. Cambridge University Press, Cambridge.

Stanley, G., and B. van de Schootbrugge. 2018. The evolution of the coral–algal symbiosis and coral bleaching in the geologic past. Pp. 9–26 *in* M. J. H. van Oppen and J. M. Lough, eds. *Coral bleaching: patterns, processes, causes and consequences*. Springer, Berlin.

Stanley, G. D. 2003. The evolution of modern corals and their early history. *Earth-Science Reviews* **60**:195–225.

Stanley, G. D., and K. P. Helmle. 2010. Middle Triassic coral growth bands and their implication for photosymbiosis. *Palaios* **25**:754–763.

Stanley, G. D., Jr., and P. K. Swart. 1995. Evolution of the coral-zooxanthellae symbiosis during the Triassic: a geochemical approach. *Paleobiology* **21**:179–199.

Sturaro, N., Y. E. Hsieh, Q. Chen, P. L. Wang, and V. Denis. 2021. Trophic plasticity of mixotrophic corals under contrasting environments. *Functional Ecology* **35**:2841–2855.

Vilhena, D. A., and A. B. Smith. 2013. Spatial bias in the marine fossil record. *PLoS ONE* **8**:e74470.

Voje, K. L. 2018. Assessing adequacy of models of phyletic evolution in the fossil record. *Methods in Ecology and Evolution* **9**:2402–2413.

Wood, S. N. 2017. *Generalized additive models*. Chapman and Hall/CRC, Boca Raton, Fla.

Zapalski M. K., J. Nowicki, M. Jakubowicz, and B. Berkowski. 2017. Tabulate corals across the Frasnian/Famenian boundary: architectural turnover and its possible relation to ancient photosymbiosis. *Palaeogeography, Palaeoclimatology, Palaeoecology* **487**:416–429.